Fragile-to-strong crossover coupled to the liquid-liquid transition in hydrophobic solutions

D. Corradini, P. Gallo, S. V. Buldyrev, and H. E. Stanley

Phys. Rev. E **85**, 051503 — Published 9 May 2012

DOI: 10.1103/PhysRevE.85.051503

Fragile to strong crossover coupled to liquid-liquid transition in hydrophobic solutions

D. Corradini

Center for Polymer Studies and Department of Physics,

Boston University, 590 Commonwealth Avenue,

Boston, Massachusetts 02215, USA

P. Gallo*

Dipartimento di Fisica, Università Roma Tre,

Via della Vasca Navale 84, I-00146 Roma, Italy

S. V. Buldyrev

Department of Physics, Yeshiva University,

500 West 185th Street, New York, New York 10033, USA

H. E. Stanley

Center for Polymer Studies and Department of Physics,

Boston University , 590 Commonwealth Avenue,

Boston, Massachusetts 02215, USA

(Dated: 30 March 2012 Revision — **LM13368E**)

Abstract

Using discrete molecular dynamics simulations we study the relation between the thermodynamic and diffusive behaviors of a primitive model of aqueous solutions of hydrophobic solutes consisting of hard spheres in the Jagla particles solvent, close to the liquid-liquid critical point of the solvent. We find that the fragile-to-strong dynamic transition in the diffusive behavior is always coupled to the low-density/high-density liquid transition. Above the liquid-liquid critical pressure, the diffusivity crossover occurs at the Widom line, the line along which the thermodynamic response functions show maxima. Below the liquid-liquid critical pressure, the diffusivity crossover occurs when the limit of mechanical stability lines are crossed, as indicated by the hysteresis observed when going from high to low temperature and vice versa. These findings show that the strong connection between dynamics and thermodynamics found in bulk water persists in hydrophobic solutions for concentrations from low to moderate, indicating that experiments measuring the relaxation time in aqueous solutions represent a viable route for solving the open questions in the field of supercooled water.

PACS numbers: 64.70.Ja,65.20.-w,66.10.C-

* gallop@fis.uniroma3.it

I. INTRODUCTION

Over the past decade our understanding of the puzzling behavior of water in the supercooled region has greatly expanded [1]. At present, plausible scenarios that might fill in the missing pieces of our comprehension have been developed through simulations and theoretical models. In 1992, using a molecular dynamics simulation of the ST2 potential, the existence of a liquid-liquid critical point (LLCP) in the supercooled region of water was hypothesized [2]. Since that time the LLCP has been found in a number of other simulations [3–5]. In this conceptual framework the presence of the LLCP explains the puzzling anomalies in the behavior of water. Although the LLCP scenario remains fascinating, its existence has not been experimentally confirmed, and alternative scenarios have been proposed [6]. Experiments are consistent with the existence of a LLCP [7, 8] but proof has been difficult because efforts to reach the zone in the phase diagram where the LLCP would be located are hampered by nucleation. On the low temperature side the existence of high density amorphous (HDA) and low density amorphous (LDA) states with a first-order coexistence line separating them has been experimentally proven [9]. If a LLCP exists, it is at the terminating point of the extension of this line in the supercooled liquid region. [8, 10].

In 1996 a strong relationship between the dynamic and thermodynamic behaviors of water was reported [11], indicating that the well-known singular temperature T_S at which various thermodynamic and dynamic anomalies diverge, can be identified with the crossover temperature T_C of the mode coupling theory [12]. This crossover temperature marks the fragile-to-strong (FTS) transition that occurs in supercooled liquids approaching the glass transition. Recent studies have completed the picture for water by connecting this FTS transition to the crossing of the "Widom line" [4, 13, 14]. Upon approaching the LLCP, the lines of maxima of the different response functions converge on this Widom line, which separates water with HDL-like features at high temperatures from water with LDL-like features at low temperatures [14, 15].

Simulations have indicated that the LLCP persists in aqueous solutions for concentrations ranging from low to moderate both for polar and apolar solutes [5, 16–19]. This suggests that focusing on aqueous solutions might be a possible experimental strategy in probing the existence of a LLCP. In solutions, in fact, the nucleation barrier can be tuned and brought below the LLCP [5, 17]. Very recently experiments on water/glycerol mixtures [20] have

shown signs of a liquid-liquid phase transition. Nonetheless, thermodynamic measurements are more difficult than measurements on dynamics, therefore it is timely to prove whether the FTS crossover remains coupled to the liquid-liquid transition also in aqueous solutions, as this can address the experimental quest on the existence of LLCP toward the study of dynamics. We note that it is a priori not obvious that the FTS transition transfers to aqueous solutions as it is a phenomenology present in many glass formers that do not have a LLCP. In this paper we use a primitive model able to reproduce the phenomenology of water. We present the results of discrete molecular dynamics (DMD) simulations on water mixed with hard spheres (HS), in order to determine whether the connection between dynamics and thermodynamics retains its validity in hydrophobic solutions.

The paper is structured as follows. Simulation details are reported in Sec. II. The results are presented and discussed in Sec. III. Concluding remarks are given in Sec. IV.

II. SIMULATION DETAILS

The primitive model used for the results presented in this paper is the Jagla model [21] [see Fig. 1(a)], an isotropic potential with two length scales, a hard-core distance a and a soft-core distance b, plus an attractive ramp that extends to a cut-off distance c. The parameterization we use, $b/a = 1.72$, c/a=3 and $U_R/U_0 = 3.56$, has been shown to possess bulk water anomalies and a liquid-liquid transition [4, 22]. The Jagla model was also successful in reproducing the increase of solubility upon cooling of non-polar solutes modeled as HS [23, 24].

Physical quantities are expressed in reduced units [18]. The total number of particles contained in the cubic simulation box is $N = 1728$. We performed DMD simulations on the discretized version of the Jagla ramp potential, for the bulk and for $x_{\rm HS} = 0.10$ and $x_{\rm HS} = 0.15$ HS(J) mixtures of HS in Jagla particles, at constant N, P and T. Pressures and temperatures are controlled by Berendsen algorithms. The HS have diameter a and the same mass as the Jagla particles. Solute-solute and solute-solvent interactions are purely hard-core. The position of the LLCP of the bulk Jagla system [4, 22, 25] and of HS(J) mixtures with mole fraction up to $x_{\rm HS} = 0.50$ has been previously determined [18] in NVT simulations. Its position in the $P-T$ plane shifts to higher pressures and lower temperatures upon increasing the mole fraction of HS. In the Jagla model the slope of the liquid-liquid

coexistence line is positive, unlike other models for water [1]. Consequently the HDL is the more ordered phase and has an Arrhenius dynamic behavior, while the reverse is true for other models [4, 18, 22]. Simulations with primitive models have the advantage of permitting to explore for large systems, a wide range of pressures and temperatures, especially in the deep supercooled region, where equilibration of long-range, orientational dependent potentials becomes impossible. In particular, the ramp potential with the choice of parameters used here is able to reproduce, *mutatis mutandis*, the complex thermodynamic scenario of water commonly derived from long-range orientational dependent potentials [2, 3, 5].

III. RESULTS AND DISCUSSION

In order to verify the connection between dynamic and thermodynamic behaviors, we consider the phase diagrams of bulk water and aqueous solutions previously determined for the Jagla potential and we study the thermodynamic and diffusive behavior along constant pressure paths [see Fig. 1(b)]. In particular, we consider isobaric paths near and above the LLCP, at the LLCP, and near and below the LLCP. Paths α, β, and γ are above the critical pressure and cross the Widom line. The path δ is at the critical pressure. Paths ϵ and ϵ' are below the critical pressure, and cross the HDL and LDL limit of mechanical stability (LMS) lines depending on the direction. In particular, along path ϵ the system goes from LDL (high T) to HDL (low T) when crossing the LDL LMS while along path ϵ' it goes from HDL to LDL upon crossing the HDL LMS. Path ζ, also below the critical pressure, does not cross the LDL LMS line and therefore the system remains in the LDL all along the path. All paths, except path ϵ', have been performed starting from a configuration at high temperature and progressively equilibrating the system at lower temperatures. For path ϵ' the starting configuration was taken at low temperature and the system was progressively equilibrated at increasing temperatures in order to cross also the HDL LMS.

Figure 2 shows the behavior of the isobaric specific heat $C_P \equiv (1/N) \cdot (\partial H/\partial T)_P$ for bulk water and for the $x_{\rm HS} = 0.15$ HS(J) solution calculated for all the paths shown in Fig. 1(b). The results for the $x_{\rm HS} = 0.10$ HS(J) solution follow a similar trend and are not shown. Both in bulk water and in the solutions, the points above the critical pressure at which the specific heat displays a maximum define the Widom line emanating from the LLCP. Consistent with the positive slope of the liquid-liquid coexistence line for the

Jagla potential [4, 22], the specific heat maximum moves to a higher temperature as the pressure increases. Its height decreases moving away from the LLCP. For the paths along the critical pressure, the temperature of the maximum falls close to the one estimated in NVT simulations [18, 22]. We note that paths ϵ and ϵ' clearly show the hysteresis expected for a first-order transition in a finite size system with the C_P maxima occurring at different temperatures, one corresponding to the LDL LMS for path ϵ and one corresponding to the HDL LMS for path ϵ'. Along path ζ, which does not reach the LDL LMS, no peak is observed.

We now show the diffusive behavior of Jagla particles in solution along the same constant pressure paths and compare it with the bulk Jagla results. Figure 3 shows the diffusion coefficient as a function of inverse temperature for bulk Jagla particles and $x_{\rm HS} = 0.10$ and 0.15 HS(J) solutions. For all three systems, above the LLCP the diffusion coefficient shows a crossover as it crosses the Widom line as determined from the C_P maxima. Along path ζ, that does not cross the LDL LMS line, the temperature dependence of D is clearly non-Arrhenius, indicating that the LDL liquid can be classified as fragile. Taking advantage of this particular potential we could push this path to very low temperatures and thus observe a clear fragile behavior. In Fig. 3 we also show the fit to the Vogel-Fulcher-Tamman, VFT, function $D = D_0 \exp[-B/(T - T_0)]$ characterizing the fragile behavior of a glass former.

For all the paths crossing the Widom line, on the high temperature side of this line we find a LDL-like liquid, and the diffusive behavior is that of a fragile liquid, when compared to path ζ who is always in the LDL fragile environment. On the low temperature side of the Widom line the diffusive behavior shows a steep straight slope typical of a strong liquid with D following the Arrhenius law, $D = D_0 \exp(-E_A/k_B T)$.

Along paths δ, at the critical pressure the diffusivity jumps from high-temperature fragile behavior to low-temperature strong behavior close to the estimated temperature of the LLCP. An analogous jump is found when crossing the LDL LMS line along paths ϵ. We note that the jump appears only when passing the LLCP or a LMS line. In analogy with the hysteresis behavior observed for the isobaric specific heat (see Fig. 2), a jump is also observed when heating up the systems along paths ϵ', but now it occurs at a temperature corresponding to the HDL LMS line. This indicates that the hysteresis caused by the first-order transition observed when studying the thermodynamic behavior in a finite system is observed for the diffusive behavior as well. This jump in the diffusion coefficient is a

finding that can be useful for the experimental determination of the liquid-liquid coexistence. These findings confirm the coupling between the dynamic and the thermodynamic behavior observed in bulk water ($P > P_c$ corresponds to $P < P_c$ and vice versa in other models [26] for the reversed slope of the coexistence line) and extends its validity to hydrophobic solutions.

Figure 4 shows the LLCP, HDL, and LDL LMS lines, the points at which the isobaric specific heat C_P and coefficient of thermal expansion α_P maxima occur and the points at which a crossover in the diffusive behavior is found. The coefficient of thermal expansion $\alpha_P = (1/V) \cdot (\partial V/\partial T)_P$ has been calculated for all our systems and for all paths. It displays a behavior qualitatively equivalent to that of the isobaric specific heat (not shown). Above the LLCP along the Widom line C_P and α_P exhibit maxima, and the temperature at which the diffusivity crossover occurs, estimated from the derivative of the logarithm of D with respect to $1/T$, coincides with C_P and α_P temperature maxima and thus with the Widom line. The maxima in thermodynamic response functions and the diffusivity crossover at the critical pressure are also found close to the LLCP temperature, estimated in NVT simulations [18, 22]. Below the LLCP and along paths ϵ and ϵ' the points where C_P and α_P and the diffusivity crossover occur also coincide, and they correspond to the crossing of the LDL LMS line and the HDL LMS line, respectively. This shows that the hysteresis expected for the thermodynamic quantities calculated along paths ϵ and ϵ' due to the first-order coexistence line between LDL and HDL and observed only at the LMS lines due to the metastability of the phases, is also maintained in the diffusive behavior.

IV. CONCLUSIONS

Our results suggest that the FTS dynamic transition reported for water in different environments in the literature [4, 11–13, 15] occurs at the same time as the thermodynamic liquid-liquid transition. They are, in other words, two sides of the same coin and, when the isobaric paths do not cross the LMS or the Widom line, there is no crossover and the dynamic behavior remains strong or fragile. We note that this connection between dynamic and thermodynamic behaviors might be a general feature of network-forming liquids, e.g., a similar picture is found in silica [27]. Why the FTS dynamic crossover is also commonly found in glass formers [28] when it is not associated to a liquid-liquid transition remains an open question. Our results show that for moderately concentrated solutions the changes

induced by the solutes are continuous and the FTS crossover remains coupled to the liquid-liquid transition paving the way to the experimental exploration of aqueous solutions as tools to understand the mysteries of water. In particular light scattering and neutron scattering experiments [29] can be used to detect the liquid-liquid transition in aqueous mixtures. Particularly important would be to see the jump in relaxation times below the LLCP as it is directly connected to the liquid-liquid transition.

ACKNOWLEDGEMENTS

DC and PG gratefully acknowledge the computational support received by the INFN RM3-GRID at Roma Tre University. SVB acknowledges the partial support of this research through the Dr. Bernard W. Gamson Computational Science Center at Yeshiva College. HES thanks the NSF Chemistry Division for support (grants CHE-0404673, CHE 0911389 and CHE 0908218)

---

[1] P. G. Debenedetti and H. E. Stanley, Phys. Today **56**, 40 (2003); P. G. Debenedetti, J. Phys.: Condens. Matter **15**, R1669 (2003); O. Mishima, Proc. Jpn. Acad. Ser. B **86**, 165 (2010).

[2] P. H. Poole, F. Sciortino, U. Essmann and H. E. Stanley, Nature **360**, 324 (1992).

[3] P. H. Poole, F. Sciortino, U. Essmann and H. E. Stanley, Phys. Rev. E **48**, 3799 (1993); P. H. Poole, I. Saika-Voivod and F. Sciortino, J. Phys.: Condens. Matter **17**, L431 (2005); Y. Liu, A. Z. Panagiotopoulos and P. G. Debenedetti, J. Chem. Phys. **131**, 104508 (2009); M. Yamada, S. Mossa and H.E. Stanley and F. Sciortino, Phys. Rev. Lett. **88**, 195701 (2002); D. Paschek, Phys. Rev. Lett. **94**, 217802 (2005); J. L. F. Abascal and C. Vega, J. Chem. Phys. **133**, 234502 (2010); ibid. **134**, 186101 (2001); F. Sciortino, I. Saika-Voivod and P. H. Poole, Phys. Chem. Chem. Phys. **13**, 19759 (2011).

[4] L. Xu, P. Kumar, S. V. Buldyrev, S.-H. Chen, P. H. Poole, F. Sciortino and H. E. Stanley, Proc. Natl. Acad. Sci. USA **102**, 16558 (2005).

[5] D. Corradini, M. Rovere and P. Gallo, J. Chem. Phys. **132**, 134508 (2010).

[6] S. Sastry, P. G. Debenedetti, F. Sciortino and H. E. Stanley, Phys. Rev. E **53**, 6144 (1996); H. E. Stanley and J. Teixeira, J. Chem. Phys. **73**, 3404 (1980); C. A. Angell, Science **319**,

582 (2008); K. Stokely, M. G. Mazza, H. E. Stanley and G. Franzese, Proc. Natl. Acad. Sci. USA **107**, 1301 (2010).

[7] Y. Zhang, A. Faraone, W. A. Kamitakahara, K.-H. Liu, C.-Y. Mou, J. B. Leão, S. Chang, and S.-H. Chen, Proc. Natl. Acad. Sci. U.S.A. **108**, 12206 (2011); D. Banarjee, S. N. Bhat, S. V. Bhat and D. Leporini, Proc. Natl. Acad. Sci. U.S.A. **106**, 11448 (2009).

[8] O. Mishima and H. E. Stanley, Nature **392**, 164 (1998); ibid. **396**, 329 (1998).

[9] O. Mishima, J. Chem. Phys. **100**, 5910 (1994); K. Winkel, M. S. Elsaesser and E. Mayer and T. Loerting, J. Chem. Phys. **128**, 044510 (2008); C. U. Kim, B. Barstow, M. W. Tate and S. M. Gruner, Proc. Natl. Acad. Sci. USA **106**, 4596 (2009).

[10] R. J. Speedy, P. G. Debenedetti, S. R. Smith, C. Huang and B. D. Kay, J. Chem. Phys. **105**, 240 (1996); R. S. Smith and B. D. Kay, Nature (London) **398**, 788 (1999); F. Mallamace, M. Broccio, C. Corsaro, A. Faraone, D. Majolino, V. Venuti, L. Liu, C.-Y. Mou and S.-H. Chen, Proc. Natl. Acad. Sci. USA **104**, 424 (2007).

[11] P. Gallo, F. Sciortino, P. Tartaglia and S.-H. Chen, Phys. Rev. Lett. **76**, 2730 (1996); F. Sciortino, P. Gallo, P. Tartaglia and S.-H. Chen, Phys. Rev. E **54**, 6331 (1996).

[12] W. Götze, *Complex Dynamics of Glass-Forming Liquids: A Mode-Coupling Theory* (Oxford University Press, New York, 2009).

[13] P. Gallo, M. Rovere and S.-H. Chen, J. Phys. Chem. Lett. **1**, 729 (2010); P. Kumar, G. Franzese and H. E. Stanley, Phys. Rev. Lett. **100**, 105701 (2008); P. Kumar, S. V. Buldyrev, S. R. Becker, P. H. Poole, F. W. Starr and H. E. Stanley, Proc. Natl. Acad. Sci. USA **104**, 9575 (2007).

[14] G. Franzese and H. E. Stanley, J. Phys.: Condens. Matter **19**, 205126 (2007).

[15] L. Xu, F. Mallamace, Z. Yan, F. W. Starr, S. V. Buldyrev and H. E. Stanley, Nature Physics **5**, 565 (2009).

[16] D. Corradini, P. Gallo and M. Rovere, J. Chem. Phys. **128**, 244508 (2008).

[17] D. Corradini and P. Gallo, J. Phys. Chem. B **115**, 14161 (2011).

[18] D. Corradini, S. V. Buldyrev, P. Gallo and H. E. Stanley, Phys. Rev. E **81**, 061504 (2010).

[19] S. Chatterjee and P. G. Debenedetti, J. Chem. Phys. **124**, 154503 (2006).

[20] K. Murata and H. Tanaka, Nature Materials (in press). DOI: 10.1038/NMAT3271

[21] E. A. Jagla, Phys. Rev. E **58**, 1478 (1998); J. Chem. Phys. **111**, 8980 (1999).

[22] L. Xu, S. V. Buldyrev, C. A. Angell and H. E. Stanley, Phys. Rev. E **74**, 031108 (2006).

[23] S. V. Buldyrev, P. Kumar, P. G. Debenedetti, P. J. Rossky and H. E. Stanley, Proc. Natl. Acad. Sci. USA **104**, 20177 (2007).

[24] M. Maiti, S. Weiner, S. V. Buldyrev, H. E. Stanley and S. Sastry, J. Chem. Phys. **136**, 044512 (2012).

[25] L. Xu, S. V. Buldyrev, N. Giovambattista, C. A. Angell and H. E. Stanley, J. Chem. Phys. **130**, 054505 (2009).

[26] P. H. Poole, S. R. Becker, F. Sciortino and F. W. Starr, J. Phys. Chem. B **115**, 14176 (2011).

[27] I. Saika-Voivod, P. H. Poole and F. Sciortino, Nature **412**, 514 (2001).

[28] D. V. Matyushov and C. A. Angell, J. Chem. Phys. **126**, 094501(2007); F. Romano, E. Sanz and F. Sciortino, J. Chem. Phys. **134**, 174502 (2011).

[29] L. Liu, S.-H. Chen, A. Faraone, C.-W. Yen and C.-Y. Mou, Phys. Rev. Lett. **95**, 117802 (2005).

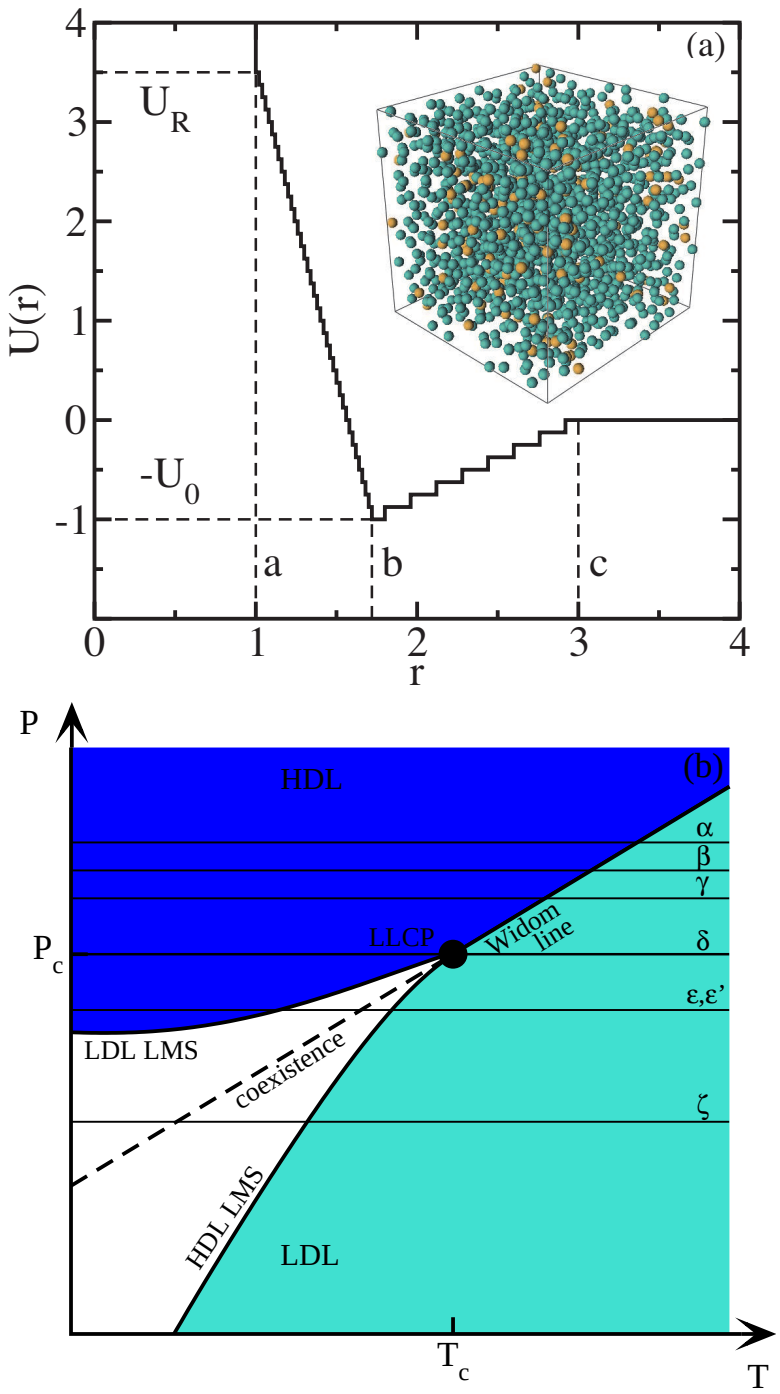

FIG. 1. (Color online) (a) Spherically symmetric Jagla ramp potential. A snapshot of the $x_{\rm HS}$ = 0.10 system is also shown in the top right corner. (b) Schematic liquid-liquid phase diagram for Jagla systems (bulk or solutions) with the LLCP and the limit of mechanical stability (LMS) lines. The constant pressure paths are simulated at $P = P_c + 0.020$ (path α); $P = P_c + 0.015$ (β); $P = P_c + 0.010$ (γ); $P = P_c$ (δ); $P = P_c - 0.010$ (ϵ) starting from high temperature; $P = P_c - 0.010$ (ϵ') starting from low temperature; $P = P_c - 0.030$ (ζ).

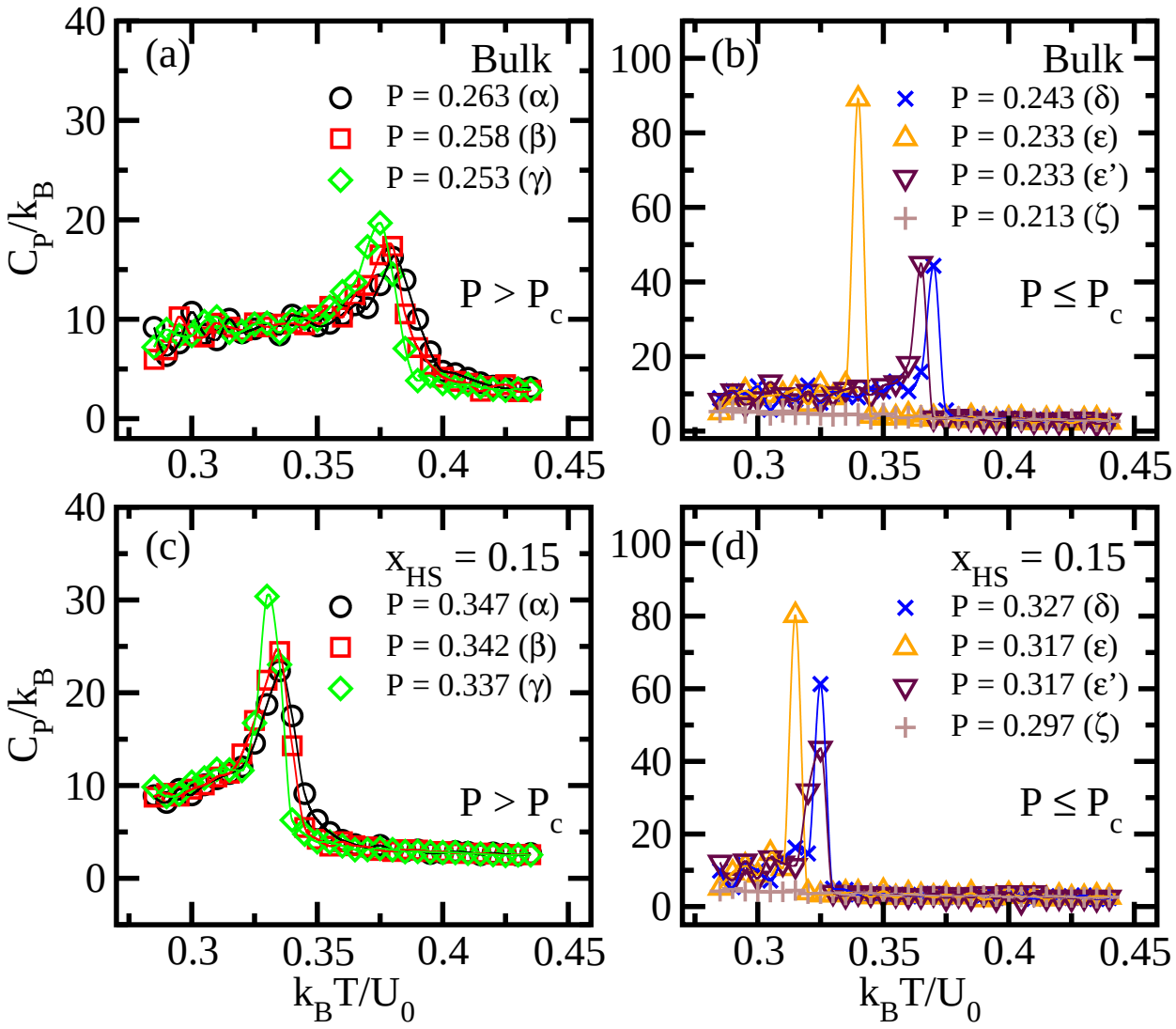

FIG. 2. (Color online) Isobaric specific heat C_P as a function of temperature (a,b) of bulk Jagla particles; (c,d) of the $x_{\rm HS} = 0.15$ HS(J) solution. Left side panels are for paths with $P > P_c$, right side panels for paths with $P \leq P_c$. Lines are cubic splines to the points.

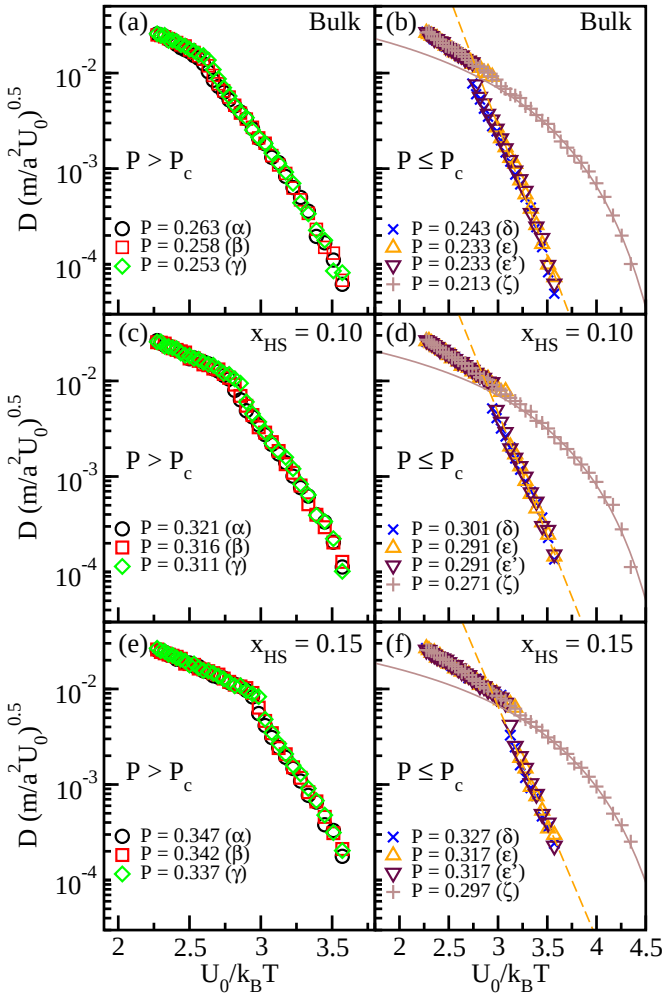

FIG. 3. (Color online) Diffusion coefficient D as a function of inverse temperature (a,b) of bulk Jagla particles; (c,d) of the $x_{\rm HS} = 0.10$ HS(J) solution; (e,f) of the $x_{\rm HS} = 0.15$ HS(J) solution. Left side panels are for paths with $P > P_c$, right side panels are for paths with $P \leq P_c$. The solid curve is a VFT fit $D = D_0 \exp[-B/(T - T_0)]$ for paths ζ. The dashed straight line is an example of Arrhenius fit $D = D_0 \exp(-E_A/k_B T)$ for paths ϵ. The parameters of the fits are $D_0 \simeq 0.4$, $B \simeq 0.25$, $T_0 \simeq 0.18$ for VFT and $D_0 \simeq 10^5$, $E_A \simeq 6$ for Arrhenius, for all systems.

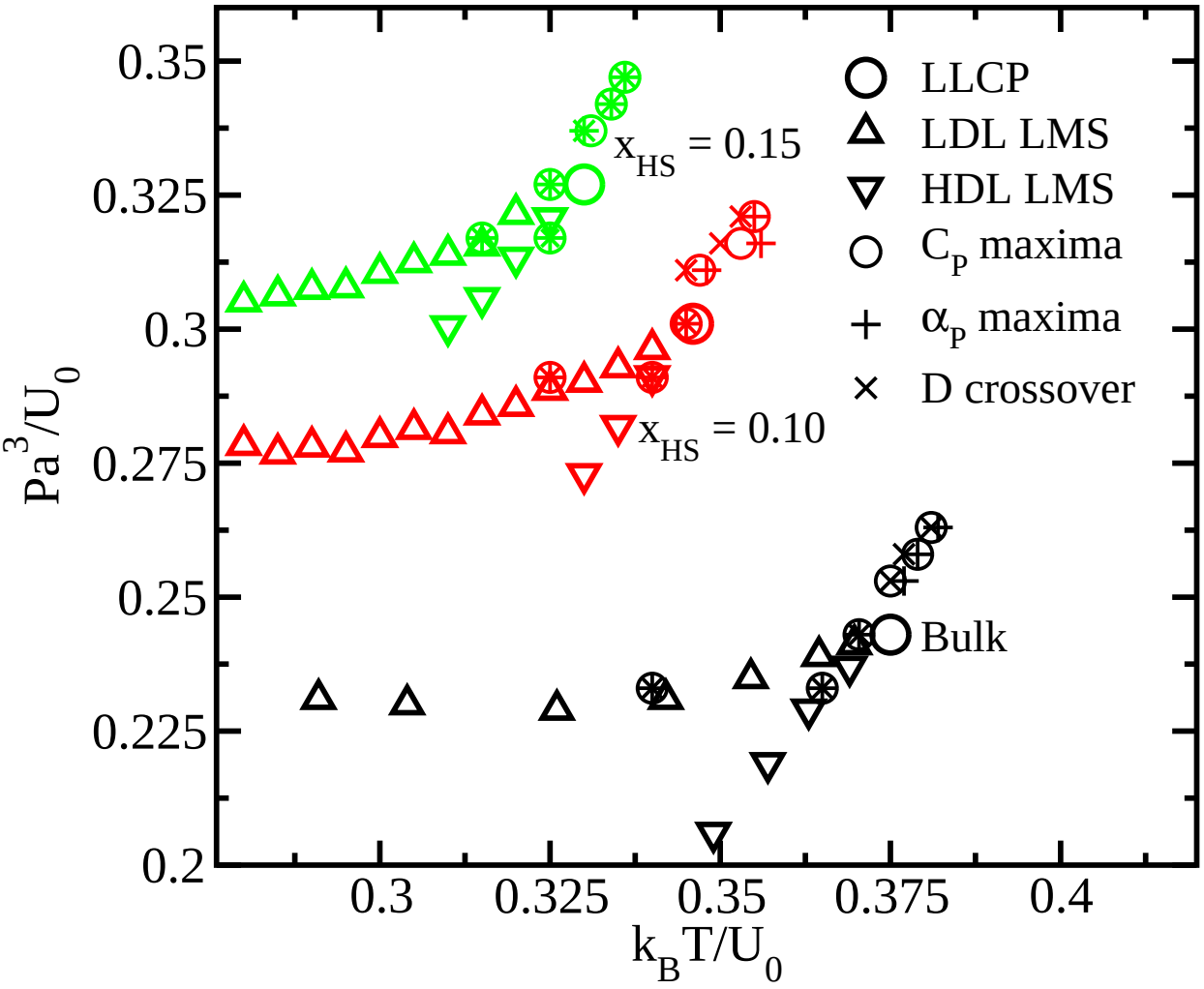

FIG. 4. (Color online) Liquid-liquid phase diagram for bulk Jagla particles, $x_{\rm HS} = 0.10$ and $x_{\rm HS} = 0.15$ HS(J) solutions. Along with the LLCP (bold large circles), LDL LMS (triangles up) and HDL LMS (triangles down), are shown the maxima of the isobaric specific heat C_P (small circles), the maxima of the coefficient of thermal expansion α_P (+) and the crossover points of the diffusion coefficient D (×).